J Mater Sci: Mater Med (2007) 18:2347–2354
DOI 10.1007/s10856-007-3135-1

Interfacial titanium oxide between hydroxyapatite and TiAlFe substrate

Valentin Nelea · Constantin Morosanu · Mircea Bercu · Ion N. Mihailescu

Received: 20 March 2006 / Accepted: 28 July 2006 / Published online: 14 June 2007
© Springer Science+Business Media, LLC 2007

Abstract The interface between nano-crystalline hydroxyapatite (HA) thin films and a titanium alloy (Ti5Al2.5Fe) has been studied by means of Fourier transform infrared spectrophotometry and X-ray diffraction at grazing incidence. The HA thin films were deposited by radio-frequency magnetron sputtering in low pressure dry argon on substrates kept at low temperature or heated at 550 °C. The effect of film treatment by sputtering and annealing in humid air, as a simple, effective way of restoring the crystallinity and stoichiometry of the HA bulk, was studied in correlation with the development of a titanium oxide layer at the film-substrate interface. An interfacial TiO_2 film grew at the interface during annealing in moist air, while a TiO_2 layer diffused into the HA films when directly sputtered at 550 °C. The formation of an interfacial titanium oxide layer was inhibited by the insertion of a crystalline TiN buffer interlayer between the substrate and the HA film. Separately, the mechanical characteristics of the different HA films were monitored by nanoindentation to find out how they had been affected.

V. Nelea · I. N. Mihailescu (✉)
National Institute for Lasers, Plasma, and Radiation Physics, P.O. Box MG-54, Bucharest 77125, Romania
e-mail: ion.mihailescu@inflpr.ro

C. Morosanu
National Institute of Materials Physics, P.O. Box MG-7, Bucharest 77125, Romania

M. Bercu
Faculty of Physics, University of Bucharest, P.O. Box MG-11, Bucharest 77125, Romania

Introduction

Hydroxyapatite ($Ca_5(PO_4)_3OH$; HA) is widely used in bone surgery and the repair of bony tissues, especially as coatings of Ti-based prostheses [1–4]. The radio-frequency (r.f.) magnetron sputtering technique has been tested for the efficient growing of thin and ultra-thin HA films on metallic substrates [5–10]. Since the deposition of highly crystalline, stoichiometric HA requires substrate processing at high temperatures in oxidizing environments, the Ti support will obviously be oxidized at the interface with the HA layer. Such harsh processing conditions lead to changes in the structure and composition of the TiO_2 passivation layer naturally existing on top of the Ti support. In these circumstances, Ti atoms or ions from the metallic bulk (sub-surface region) migrate to and inter-diffuse with the film, while oxygen migrates towards the Ti substrate from the ambient atmosphere of deposition. These dynamic multi-processes acting simultaneously at the HA–Ti border lead to the formation and development of titanium oxides that may be amorphous or crystalline, stoichiometric or nonstoichiometric [11–15]. Whereas numerous research papers have reported depositions and characterizations of HA thin films or coatings on Ti-based substrates, only a few have addressed metallic oxidation effects on HA film characteristics. Sardin et al. [12] reported that water vapor addition to an oxygen atmosphere used for pulsed laser deposition (PLD) of HA at 550 °C favored deep oxidation of the Ti substrate. Traces of TiO_2 were also found by Jelínek et al. [13] at the interface of HA thin films grown on Ti6Al4V alloys in an Ar/H_2O mixture at high temperatures (>600 °C). Fernández-Pradas et al. [14, 15] carried out analytical studies on the bioceramic-metal interface to identify potential unbeneficial or detrimental effects of interface-developed

oxides on the adhesion and mechanical performance of HA films. The authors scratch tested thick HA films that had been grown by PLD in water vapors on Ti6Al4V heated to 575 °C. According to their findings, the longer the films had been exposed to high temperature, the lower loads it took to make them fail [14]. The authors observed a layer made up of titanium oxide and a solid solution of oxygen-diffused Ti6Al4V substrate developed at the interface [15]. In the case of films grown by r.f. magnetron sputtering on substrates kept at room temperature, other authors [8] noticed an extensive outward diffusion of Ti into the HA layer and the concomitant formation of TiO_2 at or close to the interface. We too identified TiO_2 phases at the interface of a HA/Ti5Al2.5Fe system during annealing in air at 550 °C [11]. The width, structure, and chemical composition of a HA–Ti interface depend not only on the processing conditions, but also on the protocols and operational steps applied for deposition.

We present in this paper new insights into the formation and growth of interfacial titanium oxide for a HA–Ti system. The HA films were grown by r.f. magnetron sputtering technique. The influence of the titanium oxide layers on the mechanical properties of HA films was assessed.

Materials and methods

Substrate preparation

One mm-thick discs cut from a 20 mm-diameter rod of Ti5Al2.5Fe alloy (TiAlFe) were used as substrates. After mechanical polishing with wet abrasive papers of gradually decreasing grit finishes and with smooth plush cloth impregnated with a diamond suspension of up to 250 nm-diameter grains, the substrates were sequentially cleaned for 15 min in ultrasonic baths with acetone, deionized water, and ethanol. To prevent HA film contamination during further processing, some substrates were protected by coating with a 200 nm-thick TiN buffer layer. These protective films were applied by pulsed laser deposition in low pressure (10^{-1} Pa) of pure dry nitrogen on substrates heated to 650 °C [11].

HA film deposition

A 350 nm-thick HA films were deposited by r.f. magnetron sputtering at a low deposition rate of 0.28 Å s^{-1}. The radiofrequency generator operated at 1.78 MHz [10]. To improve film adhesion, all substrates were outgassed before deposition in high vacuum (10^{-3} Pa) at 250 °C for 15 min. The native titanium oxide was removed by plasma etching in argon atmosphere. The HA targets that had been obtained by cold-pressing followed by annealing in ambient air at 1100 °C were sputtered in 0.4 Pa dry argon of 99.997% purity. The target-substrate separation distance was set at 47 mm. Nanocrystalline HA films were obtained by applying either i) a substrate temperature of 550 °C (HA1 samples) or ii) a low temperature (ca. 100 °C) followed by post-deposition annealing at 550 °C in air enriched with water vapors for 1 h (HA2 samples). The substrate temperature was monitored using a thin chromel-alumel thermocouple glued with silver paste to the metallic sample surface. We further denoted by HA3 the samples deposited at high temperature (550 °C) with a TiN interlayer between the HA and substrate. Some HA films were also deposited in the same conditions as the HA2 samples, but on Si wafers instead of TiAlFe. The latter samples were prepared as controls to study the interfacial TiO_2 formation on annealing.

Film characterization

The deposited structures were investigated by grazing incidence X-ray diffraction (GIXRD), Fourier Transform Infrared Spectrophotometry (FTIR) and nanoindentation.

GIXRD measurements were carried out with a Siemens D500 diffractometer provided with a Co K_α (0.179 nm wavelength) tube. The diffractometer was equipped with Soller slits, and the post-specimen monochromator operated in parallel mode. A small copper tube having 3 mm inner diameter was placed in front of the sample in order to transform the line-shaped X-ray emission spot to a point-shaped one. The X-ray beam fell on the sample surface within a circular area of ca. 20 mm^2. In all measurements the X-ray beams were directed to the center of the depositions. To collect the diffraction signal from the film depth, the angle of incidence was gradually increased from 0.7° to 4°. A counting time of 12 sec per 0.02° step was set for each measurement. A range of 2θ angles of 25° to 70° were scanned.

The FTIR measurements were performed with a Bruker spectrophotometer in the diffuse reflectance mode at a grazing incidence of 5° within a wave-number range of 4000–500 cm^{-1}. The reflected IR beam was collected with a detector of 4 cm^{-1} resolution. A high sensitivity characterization of the samples was performed with a FTIR spectrophotometer Digilab 1100 in attenuated total reflection (ATR) mode using a ZnSe monocrystal.

The mechanical properties of the HA films were tested by nanoindentation with a Nano Indenter® XP (MTS, Corp.) apparatus equipped with a Berkovich tip. Tests were performed at maximum loads of 0.5 and 1 mN on at least 5 distinct film locations for each test and sample.

Results

GIXRD analysis

The GIXRD patterns obtained at 2° incidence angle (Fig. 1) showed that all HA samples were well crystallized. The films prevalently consisted of HA phase (card no. 9-0432 in the Powder Diffraction Files of JCPDS of ASTM), the diffraction peaks of which are indexed on the graphs. Traces of CaO lime phase (card no. 37-1497) were detected. Calcium monoxide was most probably a product of HA decomposition in the plasma during sputtering, as reported by many authors [6, 9, 10].

A crystalline TiO_2 Anatase phase was noticed in all processed HA films except those deposited with a TiN buffer layer (HA3). We note, however, that in this case, the TiO_2 phase ($2\theta = 44.54°$) could not be clearly discriminated because peaks overlapped with those of the Ti_4N_{3-x} phase ($2\theta = 44.56°$) belonging to the buffer layer. Oxygen atoms were most probably extracted from the HA plasma vapor and/or the depositing film as a result of high temperature. In addition, other oxygen atoms may have been provided by the HA film matrix and water vapors during post-deposition treatments. Titanium nitride, which appeared in the form of stoichiometric TiN, Osbornite phase, and non-stoichiometric Ti_4N_{3-x}, is known to act as an efficient diffusion barrier preventing the migration of oxygen atoms.

The mean size of the HA crystal grains was determined from the diffraction line width. Calculations were performed for (002) crystallographic planes. Their diffraction lines are intense enough and free from overlapping by other lines. All HA films were nanocrystalline with grains of ~45 nm on average, as inferred with Debye-Scherrer equation. The films that had been sputtered on substrates heated to 500 °C (HA1) showed texture along the (001) direction, while those deposited at 100 °C and annealed (HA2) exhibited a slight preferential orientation on the (100) direction.

A better insight into the interfacial TiO_2 phase was made possible by a gradual increase in grazing incidence angle during the GIXRD investigation. Figure 2 illustrates the GIXRD patterns recorded for the HA2 samples when increasing the incidence angle. The diffraction peaks characteristic of the different phases showing in the films appeared more intense as the incidence angle was increased.

As the integral diffraction signal of TiO_2 was very small for all angles used, we acquired additional quantitative information about TiO_2 growth by a comparative evaluation of the raw areas in the most prominent peaks of all phases contained in our HA–Ti system. They were: (002) HA, (004) TiO_2, (200) CaO, and (101) Ti, respectively. Diffraction signal evolutions for each phase as a function of the grazing incidence angle of the X-rays are given in Fig. 3(a) (HA1 samples) and Fig. 3(b) (HA2 samples). To discriminate between convoluted peaks, Voigt function fittings were carried out for TiO_2 and CaO.

We notice that for HA1 samples (Fig. 3a) the peak areas of HA and TiO_2 saturate at the same angle (~2°). By contrast, the TiO_2 signal still saturates at ~2° for HA2 samples (Fig 3b), but here the HA signal saturates even earlier (at ~1.2°). This indicates that TiO_2 mainly develops as a diffused layer into the hydroxyapatite film in the case of HA1 and as an interfacial layer, below the hydroxyapatite film for HA2. Similarly, CaO appears to diffuse uniformly into the film depth for HA1 samples, but penetrates deeper into the HA (near the HA–Ti interface) for samples HA2.

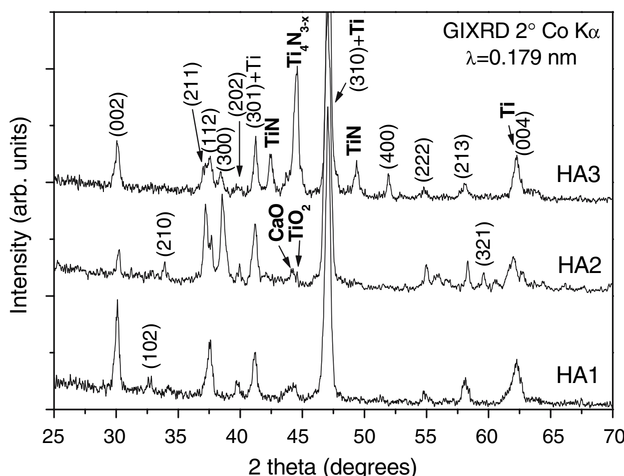

Fig. 1 Typical GIXRD patterns for samples HA1, HA2 and HA3 at 2° incidence angles of X-rays

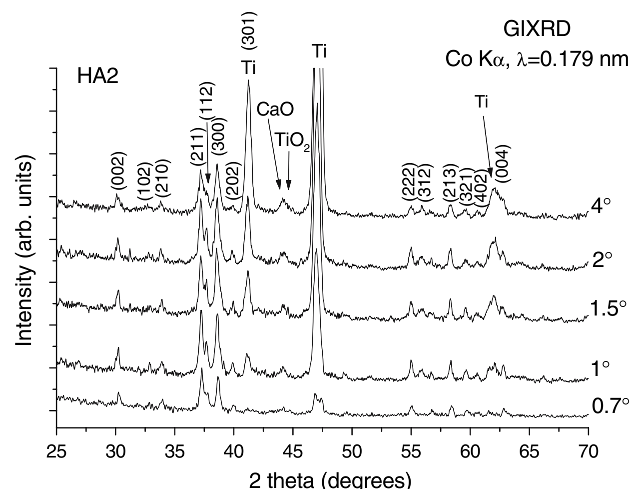

Fig. 2 Typical GIXRD patterns for annealed sample HA2 versus the incidence angle of X rays

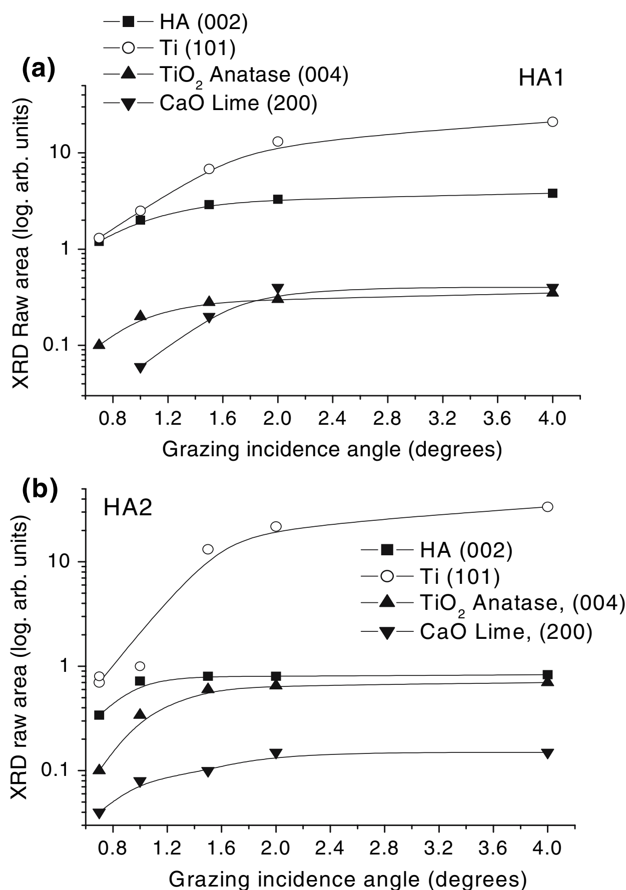

Fig. 3 Dependence of XRD raw areas on incidence angle in case of HA1 (**a**) and HA2 (**b**) samples for HA (002), CaO (200), TiO_2 (004) and Ti (101) lines

FTIR studies

Typical FTIR spectra of the HA films (Fig. 4) reveal strong vibrations at the following wave numbers: 577, 604, 961, 1024, and 1092–1117 cm^{-1}. These absorption bands are characteristic of the PO_4^{3-} orthophosphate group. The splitting of the broad absorption band centered at 590 cm^{-1} into two peaks at 604 cm^{-1} and 577 cm^{-1} originates from the bending vibrations of O–P–O bonds in the crystalline matrix of HA. The absorption band centered at 877 cm^{-1} is attributed to bending vibrations of the carbonate CO_3^{2-} ions that can easily replace PO_4^{3-} ions in the HA lattice. Stretching bands corresponding to CO_3^{2-} are located within the wide band of 1400–1500 cm^{-1}. The shifts of the absorption bands and changes in their profile for the HA film samples analyzed are determined by both a modification in the crystalline/amorphous phase ratio and local nonstoichiometry. Experimental data indicate that CO_3^{2-} incorporation in the film structure is more intense for annealed samples (HA2). Carbon bonding during annealing in humid air is the result of interaction between the as-deposited film and CO_2 molecules at 550 °C. The formation of calcium carbonate in the case of annealed samples suggests that H_2O/CO_2 adsorbed from the annealing atmosphere react with the Ca atoms in the HA films. In particular, CO_2 might react with CaO directly to form $CaCO_3$.

The broad adsorption band at 793 cm^{-1} (Fig. 4) was the subject of further careful analysis. This absorption band only appears after annealing in humid air and only for films deposited on TiAlFe. As can be seen in Fig. 5, it appears neither for the film deposited on Si, nor for the one deposited on TiAlFe at 550 °C in argon. Annealing conditions were the same for the HA samples deposited on both TiAlFe and Si. All these facts suggest that Ti in the metallic support underwent a catalytic oxidation at the interface as a result of incorporating the OH^- group during annealing at 550 °C in moisture. This process takes place simultaneously with crystalline phase formation from the initially amorphous HA film. This assertion is supported by the splitting of the broad absorption band at 590 cm^{-1} into three narrow components which was observed for all samples, without any influence from the substrate nature.

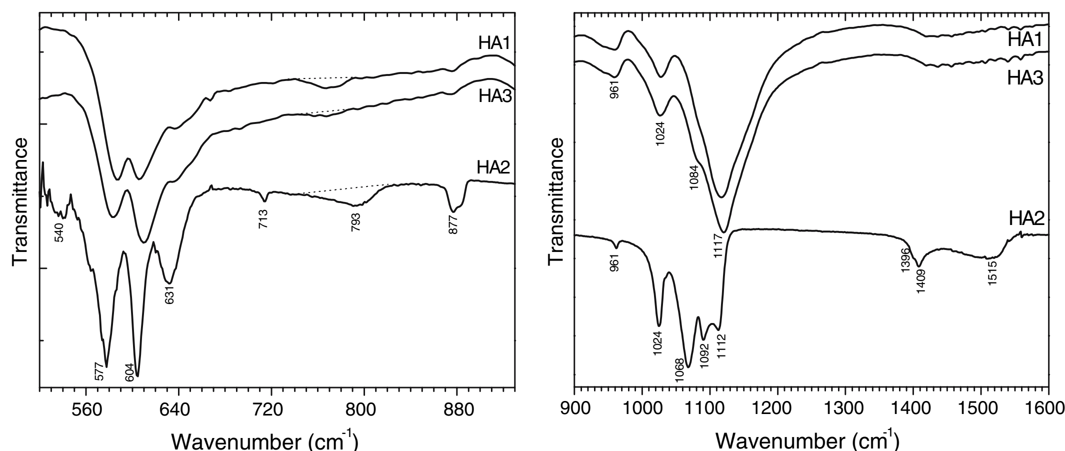

Fig. 4 Recorded FTIR spectra of HA samples in the range of 500–900 cm^{-1} and 900–1600 cm^{-1} revealing the main vibration modes

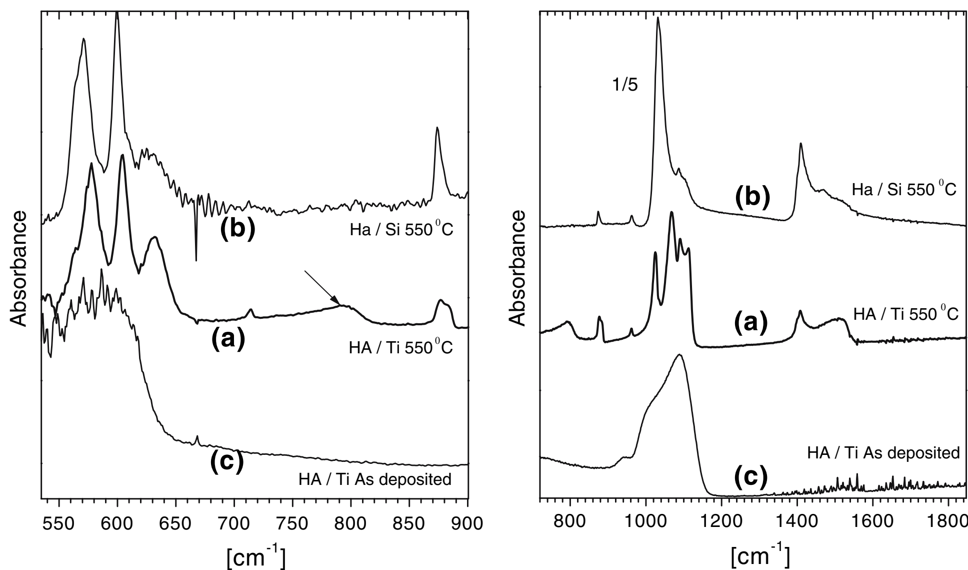

Fig. 5 Recorded FTIR spectra of HA deposited thin films onto TiAlFe and Si substrates revealing characteristic features to the titanium oxide growth at the interface between HA and the metallic substrate as a result of annealing at 550 °C in humid air

The absorption band appearing at 631 cm^{-1} after annealing is an indication of a steep increase in OH^- population bonds. It suggests that Ti oxidation at the interface was enhanced by the incorporation of OH^- groups during thermal treatment at 550 °C in humid air. XRD data are in agreement with this conclusion, certifying an increase in TiO_2 crystalline phase content in the HA samples annealed and deposited on metallic substrates (HA2). Beyond this agreement, an amorphous oxidizing phase must be assumed as taking place at the interface between the HA film and TiAlFe substrate, as a result of the potential broad variety of chemical bonds such as Ti–O–PO_3, Ti–O–P–OH, Ti–O–O–Ti [16–18], or Ti–O–OH that can be formed. FTIR spectra reveal the reported active vibration of the first and second group peaking at 712 cm^{-1} [19]. This absorption band was found for HA2 samples as part of the 700–820 cm^{-1} band centered around 793 cm^{-1} (see Fig. 5). The very low intensity of this band in the case of HA3 samples (see Fig. 4) can be attributed to the TiN buffer layer acting as an efficient barrier to prevent Ti diffusion toward the HA film. According to data in Fig 5, the absorption band around 790 cm^{-1} arises as a result of air annealing of the HA/Ti sample and is missing in the case of as-deposited HA layers on Ti based substrates. The assignment of this IR absorption band has been facilitated by comparing the spectra of the HA layer deposited on a different type of substrate such as crystalline Si (see Fig 5) with the behavior of the HA/Ti interface in case of thermal treatment at 550 °C in humid air.

Nanoindentation

The nanoindentation measurements revealed smooth, discontinuity-free, load-displacement curves. Fig. 6 shows the penetration depths of the indenter tip under 0.5 and 1 mN loads applied in 5 distinct locations on films grown with and without TiN buffer layer (HA1 and HA3 samples). At these load values, the penetration of the indenter kept shorter than one-third of HA thickness and allowed us to measure accurately the intrinsic Young's modulus and nano-hardness of the HA film [11]. The tip displacements were always smaller for HA films deposited on TiN. Indeed, the penetration depth under 0.5 mN load averaged 44 (±10) nm in films grown on TiN and increased to 64 (±10) nm for films grown on TiAlFe directly. This indicates that films deposited on TiN buffer layer are more resistant. This could be due to a higher density of the HA films having a ceramic-like interface as TiN is. The nanohardness and Young's modulus of these films were higher than 5 GPa and 130 GPa, respectively.

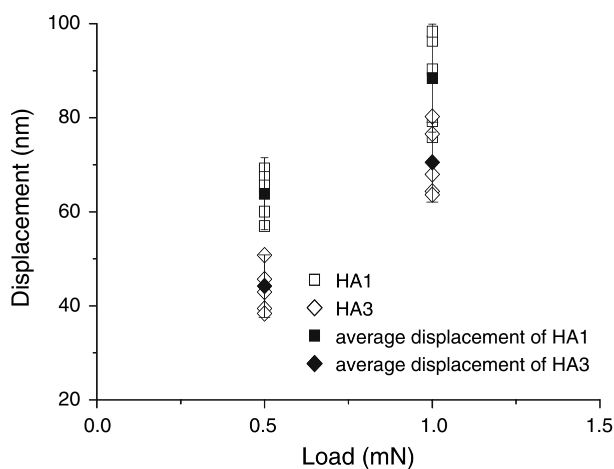

Fig. 6 Typical indenter penetration depths into HA1 films (without TiN) and HA3 (with TiN buffer layer) obtained under loads of 0.5 and 1 mN for five distinct film locations

Discussion

The oxidation kinetics of titanium generally proceed by a fast oxygen adsorption followed by a slowdown of the process until saturation is reached. More detailed investigations have shown that Ti oxidation goes through a number of events and stages [20–23]. In the early stages of exposure to O-containing atmosphere, oxygen diffuses into the Ti lattice as an interstitial agent. When oxygen dissolution into the Ti lattice has reached saturation, Ti starts to oxidize. The process gradually evolves from lower oxidation states of Ti (Ti_2O and Ti_nO_{2n-1}, where $1 \leq n \leq 10$ is an integer) to the highest oxidation state (4^+) corresponding to TiO_2. Once the TiO_2 passivation layer has been formed, it behaves as a barrier against further oxygen diffusion. Ageev et al. [21] reported that the oxidation of a thin Ti film grown on W(100) substrate started with the dissolution of oxygen atoms into its bulk up, which went on up to the limit concentration for a given temperature. The film then oxidized to TiO, with TiO_2 starting to grow when film exposure to oxygen was prolonged. Similar oxidation kinetics in ultra-high vacuum had earlier been reported by Vaquila et al. [20] for Ti thin films grown on Cu(001). Borgioli et al. [22] observed that treatments by furnace and glow-discharge processes of Ti in air at 700 °C and 900 °C resulted in a modified surface layer, essentially consisting of TiO_2 in its outer part and a rich Ti content in the interstitial atoms of the inner region. Burrell and Armstrong [23] found that a 4 nm-thick Ti_2O_3 layer developed during initial oxidation of clean polycrystalline Ti films in oxygen at 10^{-3} Pa.

Although observed by a number of authors, oxidation phenomena at the HA–Ti interface are not yet fully understood. For example it is not very clear what the formation mechanisms are, what valence and stoichiometry the oxidized-Ti has, or if the oxide is crystalline or not. Sardin et al. [12] reported that, on depositing HA on Ti at 550 °C in O_2, a weak oxidation of TiO_2 rutile and anatase occurred. In O_2/H_2O environment, a deep oxidation consisting of only TiO_2 rutile was found. Thian et al. [24] observed the formation of a crystalline TiO_2 rutile layer at the interface of Si–HA co-sputtered films on Ti after annealing in moist Ar at 700 °C. Fernández-Pradas et al. [14, 15] reported the development of an interface layer consisting of titanium oxide and a solid solution of oxygen-diffused Ti6Al4V substrate for pulsed laser-deposited HA films in water vapors at 45 Pa on 575 °C heated substrates. They showed by Raman spectroscopy that prior to the start of deposition, when water vapor and the Ti alloy kept at 575 °C were introduced, an oxygen-deficient TiO_{2-x} oxide layer was formed on the surface [14]. When a HA coating was deposited in the same conditions, an amorphous Ti_2O_3 was found at the HA–Ti alloy interface. The authors state the growing HA layer acted more as a diffusion barrier against oxygen diffusion into the substrate than as a source of oxygen for Ti oxidation. In our case, the crystalline TiO_2 anatase interfacial layer detected by XRD in films sputtered at 550 °C should appear when oxygen-containing species from the HA target reach the heated Ti surface. The sputtering took place in inert gas at a pressure 100 times lower than that used by Fernandez-Pradas et al. [14, 15]. Nieh et al. [8] reported an outward diffusion of Ti into the sputtered HA layer even at room temperature of the substrate. With the help of energy dispersive X-ray spectroscopy they found Ti atoms had penetrated about 50 nm deep into the HA layer. An interfacial TiO_2 developed, as revealed by electron energy loss spectroscopy. In our case, heating accelerated Ti diffusion and accumulation at the dynamic, growing interface.

Our XRD and FTIR data clearly revealed that the HA–TiAlFe interface was modified during processing. The interface affected by both diffusion and oxidation phenomena behaved as a compositionally and structurally complex system. XRD investigations showed that Ti was oxidized at its interface with the HA film. The oxidation mechanisms seemed to be dependent on film processing parameters. When films were grown on heated substrates, a TiO_2 crystalline layer developed due to Ti atom diffusion into the HA film. This hypothesis may explain why the TiO_2 layer appeared as if diffused in the case of HA2 layers sputtered at 500 °C for 3.5 h.

When the HA films were grown at low temperature and submitted to post-deposition annealing, the TiO_2 crystalline layer was found to be mainly localized at the interface. Our main hypothesis is that annealing makes Ti amply diffuse into the HA film and oxidize, and also drives oxygen atoms from HA and ambient air to penetrate and oxidize the first atomic layers of titanium. This TiO_2 interfacial layer develops concomitantly with the crystallization of the initially amorphous HA film. Several events may accompany this interface evolution: (i) Ti migrates from the heated bulk into the lowest layers of the HA film where it is oxidized by oxygen uptake from the amorphous HA structure; (ii) oxygen from the amorphous HA diffuses into the Ti lattice or (iii) oxygen from the moist ambient air is absorbed into the HA film, where it diffuses and reacts with Ti. Since the as-sputtered HA film has an amorphous structure at low temperature, oxygen and titanium can easily diffuse through it. A similar hypothesis has been advanced by Nieh et al. [8]. The water vapor uptake from moisture during the annealing process facilitates HA crystallization and helps preserve the hydroxyl group in the HA molecule.

Regarding the CaO minor phases observed in both films, we believe they are formed as an effect of sputtering. They might lie between the HA grains, most probably at their

boundaries or in the HA lattice interstitial sites. HA has a big molecule that can accommodate various elements or small molecules in its structure. CaO, for example, could easily occupy the OH^- sites [6, 7].

As XRD only provides information on the crystalline phases, some amorphous phases of the titanium oxides cannot be ruled out. Amorphous titanium oxide may also develop, as proven by the FTIR spectra.

Finally, we should say that due to the intricate oxidation kinetics involved in processing, it is very hard or even impossible to delimitate where the TiO_2 interfacial layer starts or ends. The interfacial diffusions of Ti into the HA film and of oxygen into the Ti bulk are competing processes. The oxidation kinetics of Ti therefore varies depending on the processing conditions (heating temperature and time, gas nature, pressure and concentration or dose) and operation protocols (order of steps).

The hardness and Young modulus of natural bone are known to depend on factors such as direction of measurement, bone type (cortical or cancellous), macro- and microstructure (lamellar, prismatic, etc.), age, hydration and mineralization, collagen fiber alignment, and organic matrix assembly, including the cells. The values of the Young modulus for the cortical bone and trabecular (cancellous) bone are 7–30 GPa and 0.05–0.5 GPa, respectively, as reported by Hench [2]. Nanoscale data gathering, mainly based on instrumented and AFM nanoindentation, is in continuous progress. In Ref. [25] it is shown that bone nanohardness ranges from 0.63 (±0.10) GPa for cancellous bone to 0.88 (±0.16) in its cortical counterpart. By comparison with values reported for natural bone, our coatings have higher nanohardness and Young's modulus, namely, 5 GPa and 130 GPa, respectively. These values guarantee site safety after implant. Indeed, the coatings should be able to support higher local stress and strains when the cells colonize them and during de-novo tissue growth.

Conclusions

This paper deals with a FTIR and GIXRD-based rapid, nondestructive, technique for characterizing the interface between HA and the titanium substrate—a most important operation if one is to ensure an adequate adhesion of biocompatible layers on the metallic substrates used in medical prosthetics. Oxidation is the main phenomenon that takes place at the interface during the technological flow. We focused on the development of a titanium oxide TiO_2 phase at the film-substrate interface as a result of substrate heating or annealing in humid air at 550 °C. We demonstrated that the TiO_2 phase developed as a rather diffused layer into the hydroxyapatite film in the case of heating during deposition and as an interfacial layer below the hydroxyapatite film in the case of post-deposition annealing. We also showed that oxidizing species in the Ti-based substrate could be kept from diffusing into the HA film by a TiN coating pre-deposited on the TiAlFe substrate. Our results indicate an approach that could improve the adherence of hydroxyapatite films deposited on Ti substrates, as medical implants strongly require. Thus, the better mechanical properties of HA films grown on TiN-coated TiAlFe substrate, combined with their successful containment of diffusion events at the interface, recommends pre-coating with TiN as an effective, affordable way to improve the adherence and performance of bioceramic coated-metallic prostheses.

Acknowledgments The authors acknowledge the financial support of the Education and Research Ministry of Romania under the contracts Biotech and CEEX ''RETEBDENT''. V. N. particularly thanks Drs. N. Broll and H. Pelletier at the National Institute of Applied Sciences (INSA) in Strasbourg, France, for access to the XRD and nanoindentation facilities, respectively.

References

1. H. AOKI, *Medical Applications of Hydroxyapatite* (Ishiyaku EuroAmerica Inc., Tokyo, St. Louis, 1994)
2. L. L. HENCH, *J. Am. Ceram. Soc.* **81**(7) (1998) 1705
3. W. SUCHANEK and M. YOSHIMURA, *J. Mater. Res.* **13**(1) (1998) 94
4. V. NELEA, M. JELÍNEK and I. N. MIHAILESCU, in *Pulsed Laser Deposition of Thin Films*, edited by R. W. EASON, Chapter 18 (Wiley, 2006) to appear
5. D. R. COOLEY, A. F. Van DELLEN, J. O. BURGESS and A. S. WINDELER, *J. Prosthet. Dent.* **67**(1) (1992) 93
6. J. G. C. WOLKE, K. Van DIJK, H. G. SCHAEKEN, K. De GROOT and J. A. JANSEN, *J. Biomed. Mater. Res.* **28** (1994) 1477
7. K. Van DIJK, H. G. SCHAEKEN, C. H. M. MAREE, J. VERHOEVEN, J. C. G. WOLKE, F. H. P. M. HABRAKEN and J. A. JANSEN, *Surf. Coat. Tech.* **76–77** (1995) 206
8. T. G. NIEH, A. F. JANKOWSKI and J. KOIKE, *J. Mater. Res.* **16**(11) (2001) 3238
9. K. OZEKI, T. YUHTA, Y. FUKUI and H. AOKI, *Surf. Coat. Tech.* **160** (2002) 54
10. V. NELEA, C. MOROSANU, M. ILIESCU and I. N. MIHAILESCU, *Surf. Coat. Tech.* **173** (2003) 315
11. V. NELEA, C. RISTOSCU, C. CHIRITESCU, C. GHICA, I. N. MIHAILESCU, H. PELLETIER, P. MILLE and A. CORNET, *Appl. Surf. Sci.* **168** (2000) 127
12. G. SARDIN, M. VARELA and J. L. MORENZA, *Deposition of Hydroxyapatite Coatings by Laser Ablation in Hydroxyapatite and Related Materials*, edited by P. W. BROWN, B. CONSTANTZ (CRC Press, Boca Raton, 1994) pp. 225–230
13. M. JELÍNEK, T. DOSTÁLOVÁ, C. FOTAKIS, V. STUDNIČKA, L. JASTRABÍK, V. HAVRÁNEK, C. GRIVAS, V. HNATOWICZ, J. KADLEC, A. PATENTALAKI, V. PEŘINA and M. POSPÍCHAL, *Laser Phys.* **6**(1) (1996) 144
14. J. M. FERNANDEZ-PRADAS, M. V. GARCIA-CUENCA, L. CLERIES, G. SARDIN and J. L. MORENZA, *Appl. Surf. Sci.* **95** (2002) 31
15. J. M. FERNÁNDEZ-PRADAS, M. V. GARCÍA-CUENCA, J. L. MORENZA, *Appl. Phys. A.* (2003)

16. H. YAMADA and J. K. HURST, *A. Chem. Soc*. **122** (2000) 5303
17. N. RYUHEI and N. N. YOSHIHIRO, *J. Am. Chem. Soc*. **126** (2004) 1290
18. K. NAKAMOTO, *Infrared and Raman Spectra of Inorganic and Coordination Compounds* (John Wiley & Sons, New York, 1986)
19. W. LIN and H. FEI, *J. Am. Chem. Soc*. **124** (2002) 9293
20. I. VAQUILA, M. C. G. PASSEGGI and JR J. FERRÓN, *Phys. Rev. B.* **55**(20) (1997) 13926
21. V. N. AGEEV, E. YU AFANAS'EVA and N. D. POTEKHINA, *Phys. Solid State.* **46**(8) (2004) 1542
22. F. BORGIOLI, E. GALVANETTO, F. P. GALLIANO and T. BACCI, *Surf. Coat. Tech*. **141**(1) (2001), 103
23. M. C. BURRELL, N. R. ARMSTRONG, *J. Vac. Sci. Tech. A*, **1**(4) (1983) 1831
24. E. S. THIAN, J. HUANG, S. M. BEST, Z. H. BARBER and W. BONFIELD, *J. Mater. Sci. Mater. Med.* **16** (2005) 411
25. G. X. NI, Y. S. CHOY, W. W. LU, A. H. W. NGAN, K. Y. CHIU, Z. Y. LI, B. TANG and K. D. K. LUK, *Biomaterials* **27**(9) (2006) 1963